JOURNAL OF SPACECRAFT AND ROCKETS
Vol. 40, No. 2, March–April 2003

Magnetohydrodynamic Control on Hypersonic Aircraft Under "Ajax" Concept

A. L. Kuranov* and E. G. Sheikin†
Hypersonic Systems Research Institute of Leninetz Holding Company, 196066, St. Petersburg, Russia

The scramjet with magnetohydrodynamic control being developed in the framework of the "Ajax" concept is considered. Model of magnetohydrodynamic generator with nonequilibrium conductivity is discussed. Simple relations for calculation of electron concentration in air plasma sustained by electron beam are proposed. A model of scramjet with magnetohydrodynamic control is considered in the one-dimensional approach. A model of inlet with magnetohydrodynamic control is considered in two-dimensional approach. It is shown that magnetohydrodynamic interaction allows one to increase specific impulse of scramjet and modify flowfield in inlet.

Nomenclature

B = magnetic induction, T
B_{cr} = critical value of magnetic induction, T
c_p = specific heat at constant pressure, J/(kgK)
c_v = specific heat at constant volume, J/(kgK)
E = electric field intensity, V/m
E_b = initial energy of electrons in e-beam, keV
e = electron charge, C
F_{th} = relative value of the inlet throat (inlet throat area divided by its full capture area)
f = Lorentz force, N/m^3
g = acceleration of gravity, m/s^2
H_u = calorific value of fuel, J/kg
h = static enthalpy, J/kg
I = e-beam induced ionization rate, m^{-3}s^{-1}, cm^{-3}s^{-1}
I_{sp} = specific impulse, s
j = current density, A/m^2
j_b = e-beam current density, A/cm^2, A/m^2
k = load factor
k_a = rate constant for attachment of electrons, m^6/s, cm^6/s
k_c = electron scattering rate constant, m^3/s, cm^3/s
k_d = rate constant for detachment of electrons, m^3/s, cm^3/s
L = length of magnetohydrodynamic generator, m
L_0 = stochiometric factor
M = Mach number
M_d = design Mach number
M_{max} = maximal flight Mach number at which internal magnetohydrodynamic generator can increase specific impulse of scramjet
M_∞ = flight Mach number
m_e = electron mass, kg
$\dot{m}$ = air mass flow, kg/s
N = gas concentration, m^{-3}, cm^{-3}
N_{O_2} = concentration of oxygen molecules in air, m^{-3}, cm^{-3}
n_e = electron concentration, m^{-3}, cm^{-3}
n_+ = positive ions concentration, m^{-3}, cm^{-3}
n_- = negative ions concentration, m^{-3}, cm^{-3}
p = pressure, Pa
q_g = power density produced by magnetohydrodynamic generator, W/cm^3, W/m^3
q_i = power density spent on ionization, W/cm^3, W/m^3
q_r = power density released in result of plasma recombination, W/m^3
R = gas constant, J/(kgK)
S_v = magnetohydrodynamic interaction parameter
T = temperature, K
t = time, s
V = volume, m^3
v = flow velocity, m/s
W_a = power transferred to magnetohydrodynamic accelerator, W
W_g = power produced by magnetohydrodynamic generator, W
W_i = ionization cost, eV
W_{ion} = power put to flow ionization in channel of magnetohydrodynamic generator, W
W_0 = total flow enthalpy, W
x, y, z = Cartesian coordinates, m
Y_e = electron stopping power in air, MeV · cm^{2}g^{-1}
α = air–fuel ratio
β = Hall parameter
β_{ci} = rate constant for electron–ion recombination, m^3/s, cm^3/s
β_{ii} = rate constant for ion–ion recombination, m^3/s, cm^3/s
γ = specific heat ratio
η_g = enthalpy extraction ratio
η_{ion} = relative power spent on flow ionization ($\eta_{ion} = W_{ion}/W_0$)
θ_N = total turning angle of flow in scramjet inlet, degree of arc
μ = electron mobility, m^2/(V · s)
ξ = factor that determines regime of magnetohydrodynamic flow
π = flow compression in inlet with magnetohydrodynamic control
π_0 = flow compression in inlet without magnetohydrodynamic control
ρ = gas density, kg/m^3, g/cm^3
σ = electrical conductivity, mho/m
σ_{in} = total pressure recovery coefficient
φ = relative air mass flow in scramjet with magnetohydrodynamic control
φ_N = nozzle nonideality factor
φ_0 = relative air mass flow in scramjet without magnetohydrodynamic control
ψ = factor which characterizes the magnetohydrodynamic generator type (Faraday or Hall)

Subscripts

x, y, z = vector projection onto corresponding axes of Cartesian coordinates

Received 5 April 2002; revision received 15 December 2002; accepted for publication 17 December 2002.

*General Director, Moskovskypz. 212.
†Head of Department.

1, 2, 3, 4, 5 = parameters at corresponding cross sections of scramjet with magnetohydrodynamic control according to Fig. 1
∞ = freestream conditions

Introduction

NOWADAYS, "Ajax" is a very popular concept of hypersonic aircraft development. It includes some basic technologies,[1] one of which is based on the use of magnetohydrodynamic (MHD) systems on the vehicle. It was shown in Refs. 2–4 that MHD interaction allows one to modify flowfield in inlet to increase specific impulse and thrust of scramjet. To realize MHD interaction, it is necessary to ensure the appreciable electric conductivity of flow. At conditions of hypersonic flight as a rule, equilibrium conductivity of a flow is negligible to produce essential MHD interaction in scramjet inlet. Thus, it is necessary to put some energy into flow to create nonequilibrium flow conductivity. It is evident that an MHD generator with nonequilibrium conductivity can be realized only in the case when the power spent on flow ionization does not exceed the power produced by the MHD generator. Such an operating mode of a system including MHD generator and ionizer we name as a self-sustained mode. Power spent on flow ionization depends on the value of conductivity needed to be created, gas-dynamic properties of flow, and type of ionizer.[3,5] Power produced by the MHD generator depends on the flow conductivity, gas-dynamic properties of flow, MHD parameters, and type of MHD generator. Thus, conditions at which the self-sustained operational mode can be realized depends on many factors, such as location of the MHD generator on the vehicle, geometry of scramjet, flight path of the vehicle, MHD parameters, ionizer type, and so on.

In this paper the requirements for parameters of the ionizer and magnetic system at which the MHD generator with nonequilibrium conductivity can be realized in hypersonic aircraft are discussed. We will take up the potential of the MHD generator to control flowfield in inlet of scramjet and to improve scramjet performance. We consider the magnetoplasma chemical engine (MPCE) under the "Ajax" concept, that is, scramjet incorporating MHD generators, located upstream of the combustion chamber, and the MHD accelerator located downstream of the combustion chamber. The simplified scheme of the MPCE is shown in Fig. 1.

MHD Generator with Nonequilibrium Conductivity

The essential component of an MHD generator with nonequilibrium conductivity is the ionizer. One of the main requirements for the ionizer is that minimal power is spent to produce the necessary conductivity of flow. Analysis of known methods of ionization shows that an electron beam is the optimal ionizer from the point of view of minimization of the power spent on ionization. According to Ref. 6, electrons with the energies greater than 1 keV spend only $W_i = 34$ eV to produce electron and ion pair in air. Ionization cost W_i in this case is only few times greater than the ionization energy of molecules of air. High-voltage pulsed discharges with the ratio of electric field strength to the gas number density $E/N > 5 \times 10^{-15}$ V · cm^{-2} are characterized by ionization cost $W_i \approx 66$ eV, according to Ref. 7. In principle, this discharge can be considered as an alternative to the e-beam.

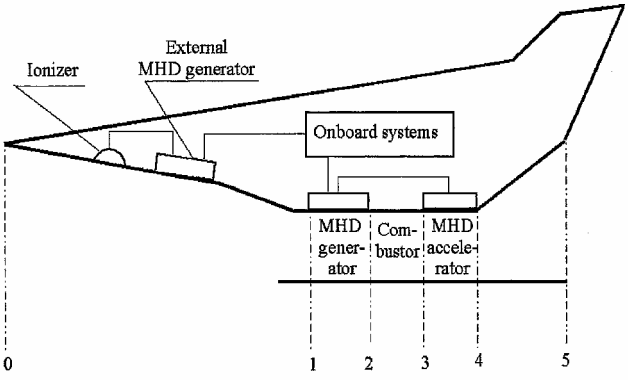

Fig. 1 Simplified scheme of magnetoplasma chemical engine.

To calculate the nonequilibrium conductivity of the flow in the channel of an MHD generator with e-beam ionizer, a model of the ionization of air was developed in Ref. 8. In the model more than 40 plasma components and more than 230 reactions of the plasma components were taking into account. Now we consider the MHD generator with nonequilibrium conductivity as a part of a complicated system, MPCE. To analyze the complex system in a wide range of parameter variations, to formulate requirements for MHD generator and ionizer, to determine optimal operational regimes of the subsystems, we need to develop a simpler model of ionization of air. Results from Ref. 8 will be used to obtain a simple approximation function for calculation of the concentration of electrons and conductivity of the flow. Also, we will consider a simple model of weakly ionized plasma consisting of neutral molecules, electrons, and negative and positive ions. The set of kinetic equations for the plasma components concentration is next:

$$\frac{\partial n_e}{\partial t} = I + k_d N n_- - k_a N_{O_2}^2 n_e - \beta_{ei} n_+ n_e$$

$$\frac{\partial n_+}{\partial t} = I - \beta_{ii} n_+ n_- - \beta_{ei} n_+ n_e$$

$$\frac{\partial n_-}{\partial t} = k_a N_{O_2}^2 n_e - k_d N n_- - \beta_{ii} n_+ n_- \qquad (1)$$

Rate constants for elementary processes taking into account the set of Eqs. (1) are functions of gas temperature and electron temperature. In calculations we use the rate constants for the processes that are listed in Ref. 9. The basic reactions are shown here:

$$e + O_2^+ \rightarrow O + O, \qquad e + N_2^+ \rightarrow N + N \qquad (2)$$

$$A^+ + B^-(+M) \rightarrow A + B(+M) \qquad (3)$$

$$e + 2O_2 \rightarrow O_2^- + O_2 \qquad (4)$$

$$O_2^- + O_2 \rightarrow e + 2O_2 \qquad (5)$$

The ionization rate I is determined in terms of e-beam characteristics by the relation

$$I = q_i / W_i \equiv (j_b/e)\rho Y_e(E_b)/W_i \qquad (6)$$

Process (3) is a two- or three-body ion–ion recombination, where A^+ and B^- are positive and negative ions, respectively. The stopping powers for electrons in various media are presented in Ref. 10. The set of Eqs. (1) practically coincides with the one from Ref. 9, except that we consider a spatially homogeneous state and we do not take into account the process $e + O_2 + N_2 \rightarrow O_2^- + N_2$ because its rate constant in our conditions is more than 50 times less than for process (4).

The concentration of electrons in nonequilibrium plasma sustained by an e-beam can be calculated numerically from the set of Eqs. (1). In the case when dissociative recombination (2) is the dominant process in the set of Eqs. (1), the steady-state electron concentration n_e, according to Ref. 3, can be approximately determined by the relation

$$n_e \approx \sqrt{q_i / W_i \beta_{ei}} \qquad (7a)$$

The ionization fraction in this case is determined by the ratio

$$n_e/N \approx \sqrt{\left(q_i / N^2\right) / W_i \beta_{ei}} \qquad (7b)$$

Figure 2 shows the dependencies of the electron concentration calculated in Ref. 8 upon the magnitude of q_i. Approximation function (solid curve) obtained for the results is given by the relation

$$n_e = 1.124 \times 10^{12} \sqrt{q_i} \cdot \text{cm}^{-3} \qquad (8)$$

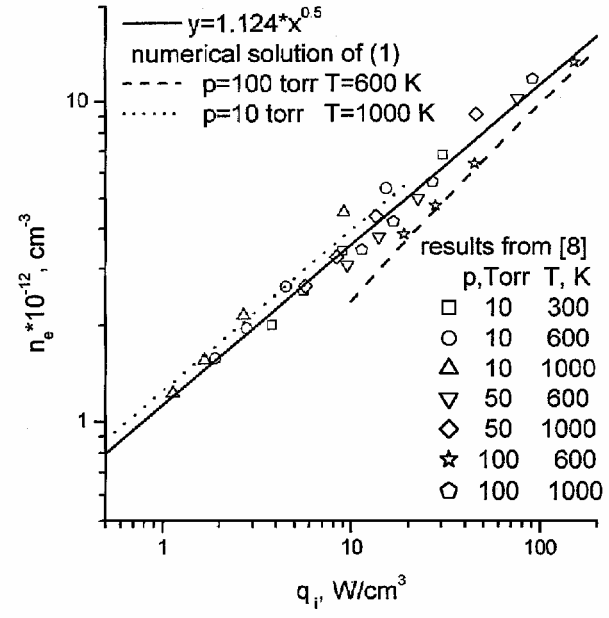

Fig. 2 Electron concentration in air plasma sustained by e-beam.

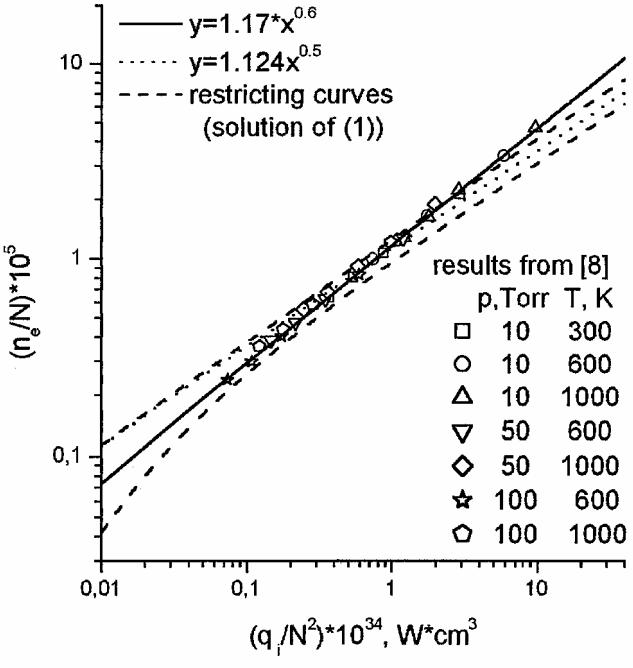

Fig. 3 Ionization fraction in air plasma sustained by e-beam.

Equation (8) coincides with Eq. (7a) at a corresponding value of the β_{ei} parameter; maximal deviation of the results of Ref. 8 from the approximation function is less than 30%. It follows from Fig. 2 that the deviations are systematic. Thus using Eq. (8) outside of the calculated ranges can result in more serious deviations. The dashed and dotted curves in Fig. 2 are steady-state solutions of Eqs. (1). These curves are in good agreement with results of Ref. 8.

Figure 3 shows the dependencies of ionization fraction of air plasma upon factor q_i/N^2. The approximation function (solid curve) obtained for the results is given by the relation

$$n_e/N = 1.17 \times 10^{-5} \times \left(10^{34} \times q_i/N^2\right)^{0.6} \qquad (9)$$

The dotted curve corresponds to relation (7b) using approximation equation (8) for n_e. Equation (9) more precisely than Eq. (7) agrees with numerical results of Ref. 8. The maximal deviation of results of Ref. 8 from approximation function (9) is less than 9%. The dashed curves in Fig. 3 are obtained as steady-state solutions of Eqs. (1).

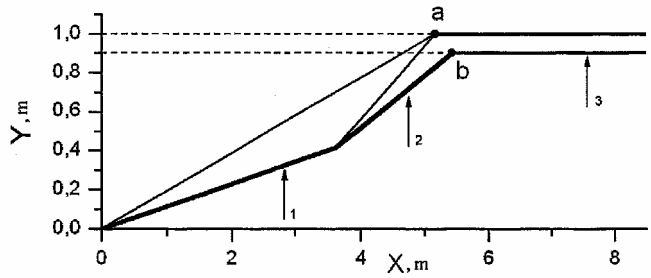

Fig. 4 Geometry of inlet of scramjet with $\theta_N = 15$ deg, $M_d = 10$, and $F_{th} = 0.1$. Individual turning angles for the inlet are 6.5 and 8.5 deg, correspondingly.

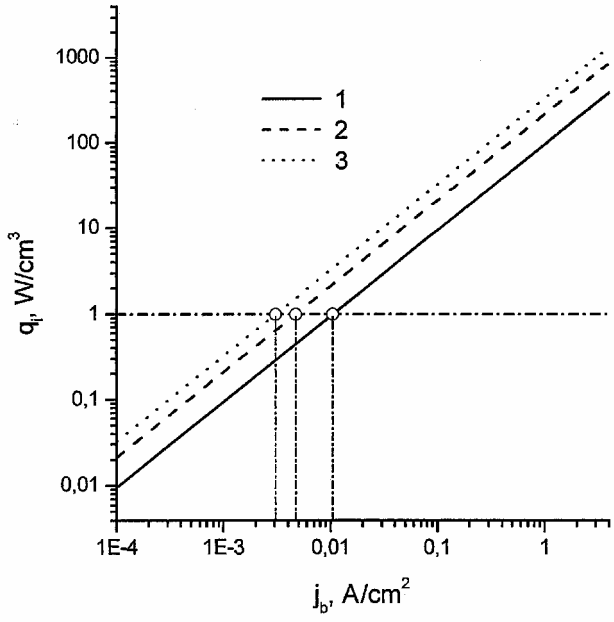

Fig. 5 Electron beam power losses in various cross sections of scramjet: $E_b = 100$ keV and $M_\infty = 8$.

They restrict the ionization fraction value for conditions in inlet of scramjet with $\theta_N = 15$ deg in the range of flight Mach number $M_\infty = 6$–10 at the freestream dynamic pressure 40 kPa. The configuration of the inlet for $M_d = 10$ is shown in Fig. 4. The individual turning angles for the inlet are 6.5 and 8.5 deg, correspondingly. Characteristic cross sections of possible locations of external and internal MHD generators are denoted in the figure. It follows from Fig. 3 that all dependencies of ionization fraction are neighbors in the range of $2 \times 10^{-2} < (q_i/N^2) \times 10^{34} < 20$. In this range formula (9) can be used with high reliability to analyze characteristics of an MHD generator with nonequilibrium conductivity.

To determine limits at which self-sustained operational mode of the ionizer and MHD generator exist, we need to compare the power density spent on flow ionization q_i and power density produced by MHD generator q_g. Power density q_g is determined by $q_g = k(1-k)\sigma(q_i)B^2v^2$. Conductivity is determined by the relation $\sigma = e^2 n_e/(m_e N k_c)$. The electron concentration n_e depends on the power density spent on flow ionization q_i. Thus power density q_g in the MHD generator with nonequilibrium conductivity is a function of q_i.

Dependencies of q_i on e-beam current density are shown in Fig. 5 in characteristic cross sections of scramjet for flight Mach number $M_\infty = 8$ with freestream dynamic pressure 40 kPa. Numbers correspond to location of the cross sections according to Fig. 4. One can see that changing the cross-section location from the first to third position causes the q_i value to be increased for a given current density.

Figure 6 shows the dependencies of power density produced by the MHD generator less the power density put into flow ionization

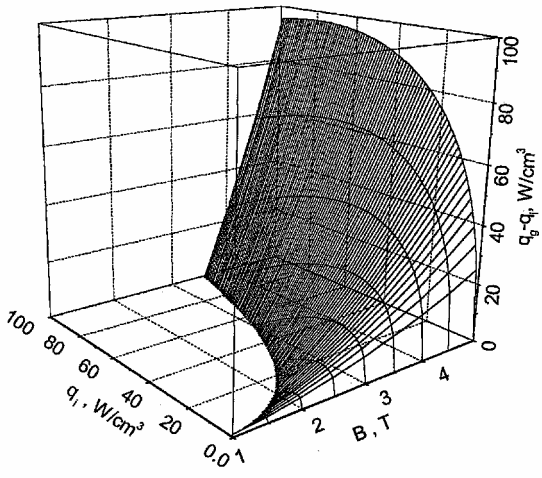

Fig. 6 Power density produced by the MHD generator less the power density put into flow ionization; $M_\infty = 6$.

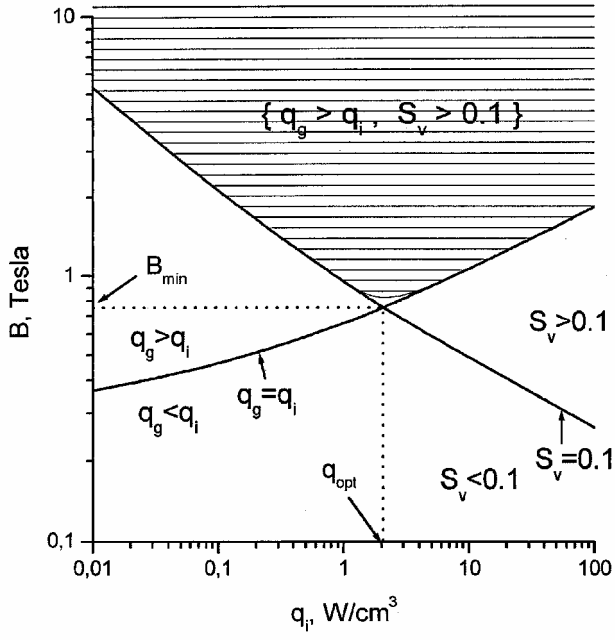

Fig. 7 Range of values of parameters that ensure the self-sustained operational mode of MHD generator located in cross section 1 (Fig. 4); $M_\infty = 6$.

$(q_g - q_i)$ as a function of q_i and B. The MHD generator is located in cross section 2 (Fig. 4). One can see that there are limiting values of magnetic induction $B = B_{cr}$ for which $q_g \geq q_i$. Increasing the value of q_i causes the critical magnetic induction to be increased. Increasing the magnetic induction at fixed q_i causes the power produced by the MHD generator to be increased. The dependence of $(q_g - q_i)$ on the q_i value is not monotonic. There is an optimal value of q_i for which $(q_g - q_i)$ has a maximum at given value of magnetic induction. In the simple case for which the electron concentration can be calculated under formula (7a), the critical value of magnetic induction is determined analytically by the relation

$$B_{cr} = \sqrt{\frac{m_e N k_c \sqrt{q_i W_i \beta_{ei}}}{[k(1-k)e^2 v^2]}}$$

It follows from the relation that critical value of magnetic induction depends on parameters of flow, the MHD generator and ionizer, and also on the rate constants of elementary processes. On the other hand, at a fixed value of B we can determine critical value of power density q_{cr} for which $q_g = q_i$. Self-sustained operational mode of ionizer and the MHD generator with nonequilibrium conductivity are realized at $q_i < q_{cr}$.

The MHD generator with nonequilibrium conductivity is a part of the MPCE, and so the electric energy production is not its only function. The MHD generator must effectively regulate characteristics of MPCE. According to the next section, to noticeably improve scramjet performance it is necessary to ensure MHD interaction parameter $S_v \geq 0.1$, where $S_v = \sigma B^2 L/\rho v$. Decreasing the power density input to ionization causes the flow conductivity to be decreased. Thus to ensure the required MHD interaction parameter while decreasing q_i it is necessary to increase magnetic induction value. The decreasing curve in Fig. 7 corresponds to constant value of MHD interaction parameter $S_v = 0.1$. The increasing curve in Fig. 7 corresponds to critical regime of the MHD generator for which $q_g = q_i$. The parameters B and q_i, which are located in the shaded area, correspond to the self-sustained operational mode of MHD generator with nonequilibrium conductivity with MHD interaction parameter $S_v > 0.1$. It follows from Fig. 7 that there is optimal value of energy input to ionization, which ensures the required regime of the MHD generator in MPCE at minimal magnitude of magnetic induction.

One-Dimensional Analysis of MPCE

To analyze the MPCE with the internal MHD generator and the MHD accelerator in a quasi-one-dimensional approach, we use the model developed in Ref. 4. The scheme we consider here is the same as shown in the Fig. 1, but the external MHD generator is absent. We consider the MHD generator with nonequilibrium conductivity. Powers spent on flow ionization W_{ion} and produced by the MHD generator W_g are determined by integrating the corresponding power densities q_i and q_g over the MHD generator volume: $W_{ion} = \int q_i \, dV$, $W_g = \int q_g \, dV$. In analysis of the MPCE, we use a dimensionless value to characterize the power produced by the MHD generator, namely, the enthalpy extraction ratio η_g. The quantities η_g and W_g are related by the ratio $W_g = \eta_g W_0$. In the case of constant value of specific heat, $W_0 = \dot{m} c_p T_1 [1 + (\gamma - \frac{1}{2}) M_1^2]$. To take into account the relative power spent on flow ionization, we introduce factor r as the ratio of power input to ionization and power produced by the MHD generator, $r = W_{ion}/W_g$. Also we will use parameter $\eta_{ion} = W_{ion}/W_0$. In general, case factor r is a function of the enthalpy extraction ratio $r = r(\eta_g)$. The function $r(\eta_g)$ can be calculated for various regimes of MHD flows on the analogy of Refs. 4 and 11, by using dependencies obtained in preceding section.

The one-dimensional model of MPCE takes into account that part $r(\eta_g)$ of the power produced by the MHD generator is put into flow ionization while the remaining power $[1 - r(\eta_g)]$ is transferred to the MHD accelerator. The power spent on flow ionization, ultimately, as a result of recombination processes passes into heat. We suppose approximately that this additional heat release is implemented in the combustion chamber. Let us consider the combustion chamber working in a mode with a constant pressure. A mass-flow rate of fuel is usually much less than air mass-flow rate; thus, we will regard a fuel supply into the combustion chamber as a heat release without injection of mass. We suppose that the nozzle flow is isentropic. The inlet implements a multishock gas-dynamical compression of the incident flow. It is characterized by the total pressure recovery coefficient σ_{in}. The engine exhaust in our consideration is perfectly expanded, so that $p_5 = p_\infty$. To take into account nozzle nonideality, we introduce factor ϕ_N. The value $\phi_N = 1$ corresponds to the ideal nozzle. In Ref. 2 it was shown that positive effect of MHD control on the specific impulse of scramjet increases while decreasing the ϕ_N value. In this paper we will consider $\phi_N = 1$.

The set of equations for calculating MPCE specific impulse I_{sp} in assumptions just listed, according to Ref. 4, is next:

$$I_{sp} = \frac{\alpha L_0}{g}(\varphi_N v_5 - v_\infty)$$

$$v_5 = \sqrt{\left(v_\infty^2 + 2c_p T_\infty\right) + 2c_p(\Delta T - T_5)}$$

$$T_5 = T_4 \Bigg/ \sigma_{in}^{(1-1/\gamma)} \left[\frac{T_1}{T_\infty}\left(\frac{T_2}{T_1}\right)^{\xi_1/\xi_1+1}\left(\frac{T_4}{T_3}\right)^{\xi_3/\xi_3+1}\right]$$

$$T_4 = T_3 + \frac{k_3 - 1}{k_3} T_\infty \left(1 + \frac{\gamma - 1}{2} M_\infty^2\right)(1 + \xi_3)\eta_g[1 - r(\eta_g)]$$

$$T_3 = T_2 + \Delta T + \frac{W_{\text{ion}}}{\dot{m} c_p}, \qquad \Delta T = \frac{H_u}{c_p(\alpha L_0 + 1)}$$

$$\frac{W_{\text{ion}}}{\dot{m} c_p} = r(\eta_g) \cdot \eta_g \cdot T_\infty \left(1 + \frac{\gamma - 1}{2} M_\infty^2\right)$$

$$T_2 = T_1 + T_\infty \left(1 + \frac{\gamma - 1}{2} M_\infty^2\right)(1 + \xi_1)\eta_g \psi$$

$$\psi = \begin{cases} \dfrac{1}{k_1} - 1, & \text{for Faraday MHD generator} \\ \dfrac{1 + \beta^2 k_1^2}{\beta^2 k_1 (1 - k_1)}, & \text{for Hall MHD generator} \end{cases} \tag{10}$$

The accordance of the factor ξ value with the typical flow regimes in the MHD channel is given in Ref. 4. Subscripts in Eqs. (10) are used to note parameters of a flow in corresponding cross sections of the engine channel according to designations indicated in the Fig. 1. Parameters T_1 and σ_{in} are determined by averaging the results of numerical calculations in the two-dimensional Euler approach. Now we briefly explain the meaning of formulas in the set of Eqs. (10). The first one is a conventional equation for scramjet specific impulse in the approach of a perfectly expanded nozzle ($p_5 = p_\infty$). The second equation determines the flow velocity at the nozzle exit in accordance with the law of energy conservation. The third equation determines the temperature at the nozzle exit. It is obtained in Ref. 3 on condition that $p_5 = p_\infty$. The last equations determine the temperature at the exits of the MHD accelerator, the combustion chamber, and the MHD generator.

The set of formulas (10) allows one to calculate specific impulse of the MPCE at given parameters of the inlet, MHD systems, and the combustion chamber. To determine the range of parameters at which the MHD interaction improves scramjet performance, we use an obvious functional ratio $(\partial I_{\text{sp}}/\partial \eta_g)|_{\eta_g \to 0} > 0$. Having done necessary transformations, it is not difficult to show that the preceding inequality is true when

$$\xi_1 > T_1/\Delta T \cdot [1 + \delta/\psi], \qquad \delta = \{1 - (1/k_3)[1 - r(0)]\} \tag{11a}$$

It is evident that $r(0)$ can be determined as the ratio of power densities $r(0) = q_i/q_g$. As $0 \le r(0) \le 1$ and $k_3 \ge 1$, the factor δ has a value in the range $0 \le \delta \le 1$. The inequality (11a) combines some parameters of the scramjet, MHD systems, and ionizer. Cursory analysis of the inequality lets us infer that the internal MHD generator allows one to increase the scramjet specific impulse only when we use the MHD generator in a regime with pressure increasing along the channel length. Indeed, for the MHD generator $\psi > 0$ and $0 \le \delta \le 1$, and so the right-hand part of Eq. (11a) is positive. According to Ref. 4, the condition $\xi_1 > 0$ corresponds to MHD flow with $dp/dx > 0$. Here we will attempt to explain clearly the physical reason for the requirement. Let us see the MPCE scheme in a situation when pressure in the channel of the MHD generator is constant. The total pressure losses in the MHD generator do not recover totally in the MHD accelerator. So the MHD interaction will decrease the scramjet specific impulse at any given heat release in a combustion chamber. The only way to improve the scramjet performance is to improve the thermodynamic cycle. The improvement of the thermodynamic

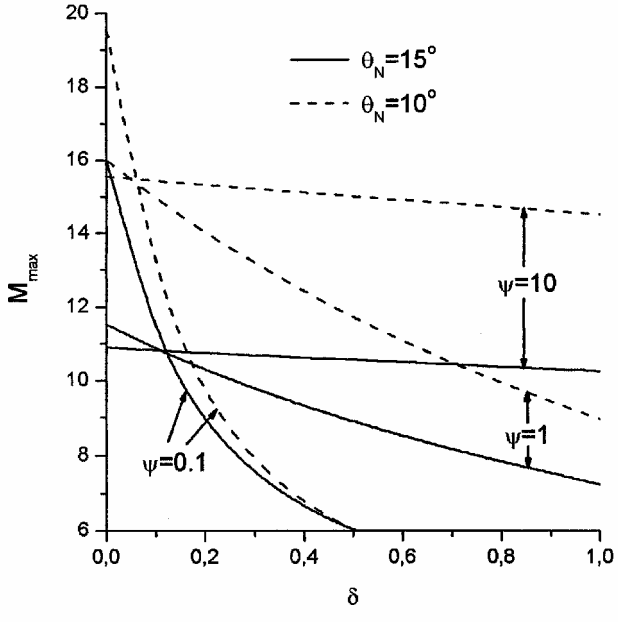

Fig. 8 Maximal Mach number for two various inlets: $M_d = 10$ and $F_{\text{th}} = 0.12$.

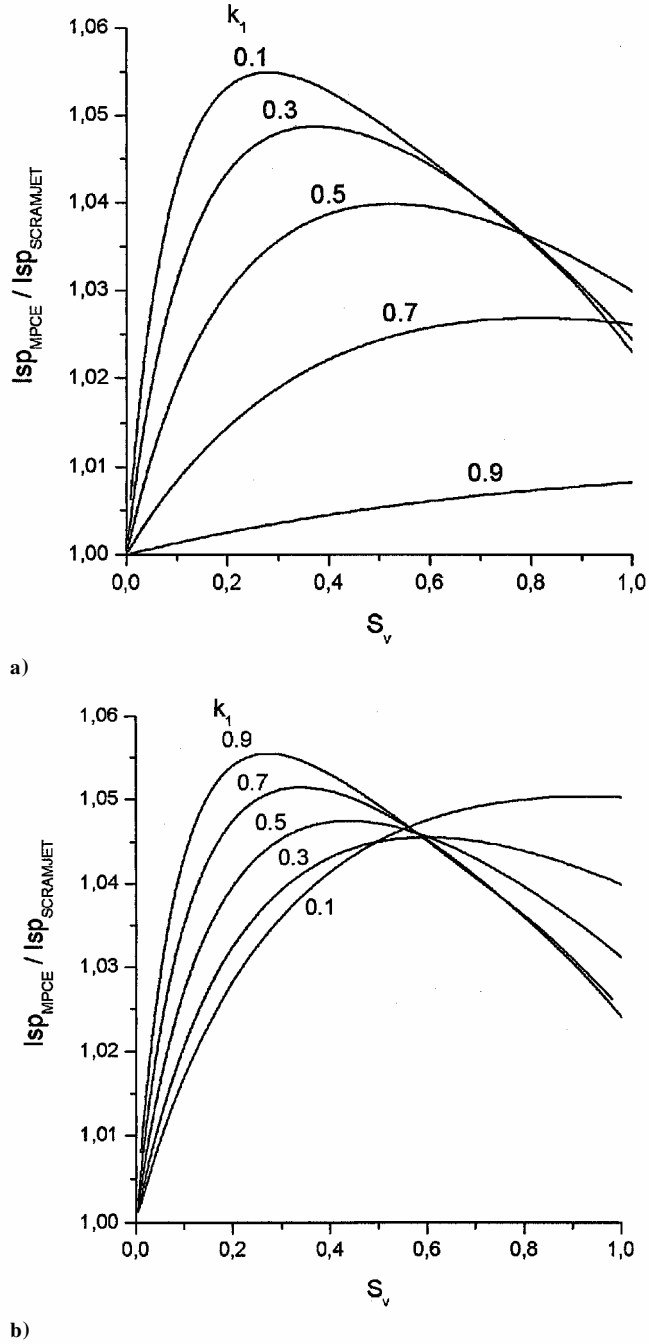

Fig. 9 Relative specific impulse of MPCE at $M_\infty = 6$, $M_d = 10$, $\theta_N = 15$ deg, $F_{\text{th}} = 0.12$, and $\delta = 0.35$: a) Faraday MHD generator and b) Hall MHD generator, $\beta = 2$.

cycle of the engine is achieved by increasing the static pressure in the MHD generator in the case when parameters of the MHD generator and the MHD accelerator satisfy inequality (11a).

If we consider the MHD generator with constant cross-sectional area, the inequality (11a) takes on the form

$$\gamma - 1 + \frac{\gamma + 1/\psi}{M_1^2 - 1} > \frac{T_1}{\Delta T} \cdot \left(1 + \frac{\delta}{\psi}\right) \qquad (11b)$$

This inequality prescribes the range of variation of MPCE subsystem parameters at which using the MHD generator with a constant cross-sectional area allows one to increase scramjet specific impulse.

As a result of inequality (11b) analysis, we obtain limitations on flight Mach number at which the MHD interaction causes the MPCE specific impulse to increase. Figure 8 shows the dependencies of maximal flight Mach number upon factor δ for various values of ψ factor. The MHD interaction increases specific impulse of scramjet in the case when flight Mach number $M_\infty < M_{\max}$. As it follows from Eq. (11a), the factor δ mainly characterizes the relative power spent on flow ionization. In situations when power spent on ionization is equal to zero (initially ionized flow), $\delta = 0$. The factor $\delta = 1$ describes the situation for which all of the power produced by the MHD generator is spent on flow ionization. It is evident that, while increasing the factor δ, $M_{\max}$ is decreasing. At a small value of δ, decreasing the ψ factor provides expansion of range of Mach-number values at which the MHD interaction improves scramjet performance. Contrarily at $\delta \approx 1$, an increase of the ψ factor causes the $M_{\max}$ to be increased.

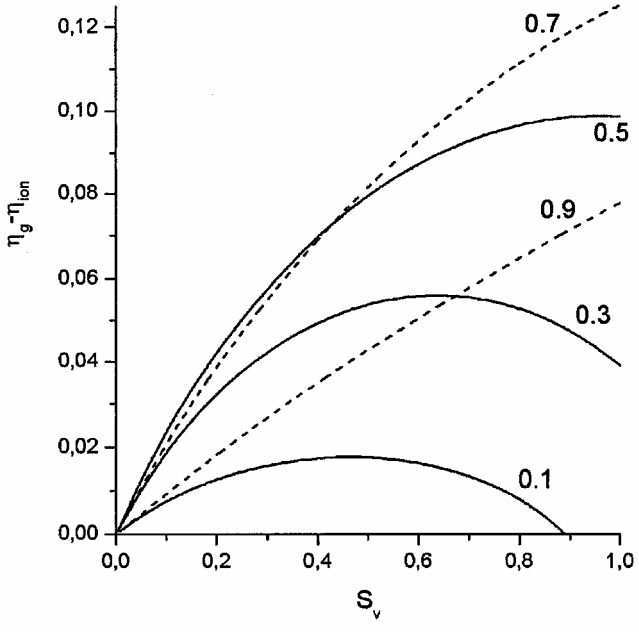

a)

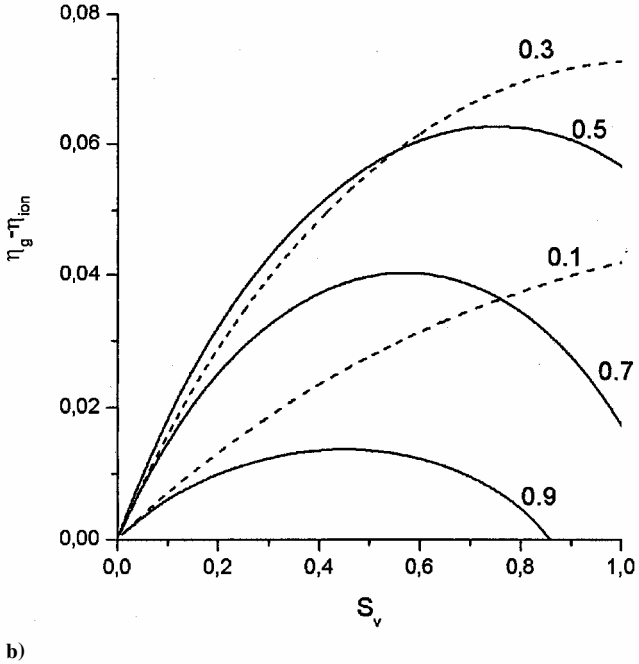

b)

Fig. 10 Relative power excess in MPCE at $M_\infty = 6$, $M_d = 10$, $\theta_N = 15$ deg, $F_{th} = 0.12$, and $\delta = 0.35$: a) Faraday MHD generator and b) Hall MHD, $\beta = 2$.

Figure 9 demonstrates how the specific impulse of the MPCE depends on the MHD interaction parameter S_v and on the load factor k_1. The load factor values are shown in Figs. 9 and 10 near the corresponding curves. In calculating we use the dependence $S_v(\eta)$ from Ref. 4. It follows from Fig. 9a that at small values of S_v parameters for a Faraday MHD generator decreasing the load factor causes the specific impulse to increase. For a Hall MHD generator (Fig. 9b) the tendency is opposite to that for the Faraday one. While increasing the MHD interaction parameter, the dependencies of specific impulse on the load factor become nonmonotone for both Faraday and Hall MHD generators. Estimations show that the Hall parameter, which is determined by the relation $\beta = \mu B$, takes on a value from 1 to 3 at typical conditions for the internal MHD generator. In calculations we consider $\beta = 2$. As it follows from Fig. 10, the dependencies of the excess power for Faraday and Hall MHD generators are quite similar. Except for to reproduce the dependency of the power excess upon load factor we need to use $k_1^{\text{Hall}} = 1 - k_1^{\text{Faraday}}$, where the upper index denotes the type of MHD generator.

Figure 11 demonstrates the dependencies of the MPCE specific impulse on the MHD interaction parameter for various relative values of the inlet throat area. One can see that the larger the inlet throat F_{th}, the greater the positive influence of the MHD interaction on the specific impulse of scramjet. For small values of S_v, the Hall MHD generator provides a more noticeable increase of scramjet specific impulse than the Faraday one. For $S_v > 0.7$ the Faraday MHD generator gives a greater increment of scramjet specific impulse than the Hall one. Figure 12 shows dependencies of the enthalpy extraction ratio for various relative values of inlet throat. One can see that the larger the inlet throat F_{th}, the greater the value η_g. The Faraday MHD generator produces more electric power than Hall one in all of the cases.

Thus we can conclude that MHD interaction improves scramjet performance only when the parameters of MPCE subsystems satisfy

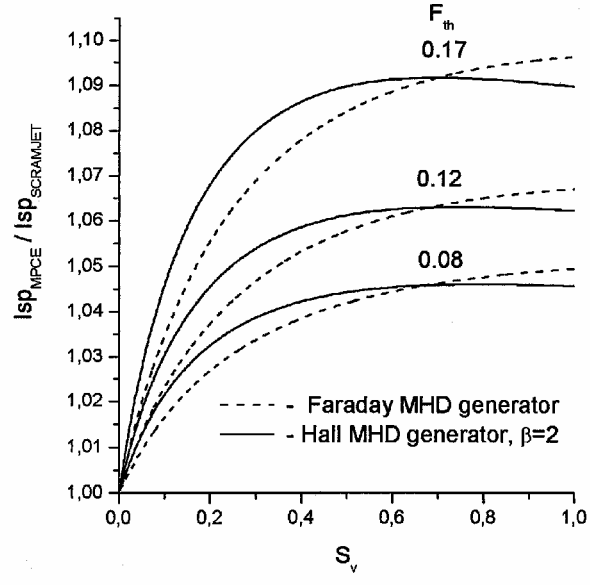

Fig. 11 Relative specific impulse of MPCE at $M_\infty = 6$, $M_d = 10$, $\theta_N = 15$ deg, $k_1 = 0.5$, and $\delta = 0.17$.

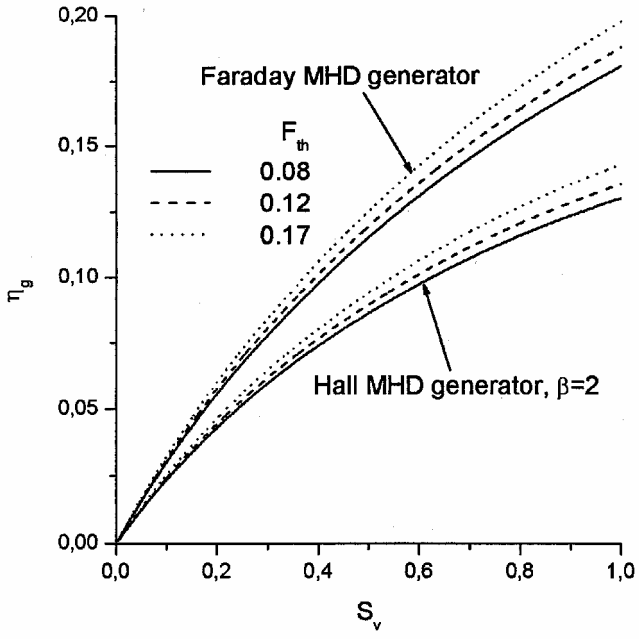

Fig. 12 Enthalpy extraction ratio for Faraday and Hall MHD generators in MPCE at $M_\infty = 6$, $M_d = 10$, $\theta_N = 15$ deg, $k_1 = 0.5$, and $\delta = 0.17$.

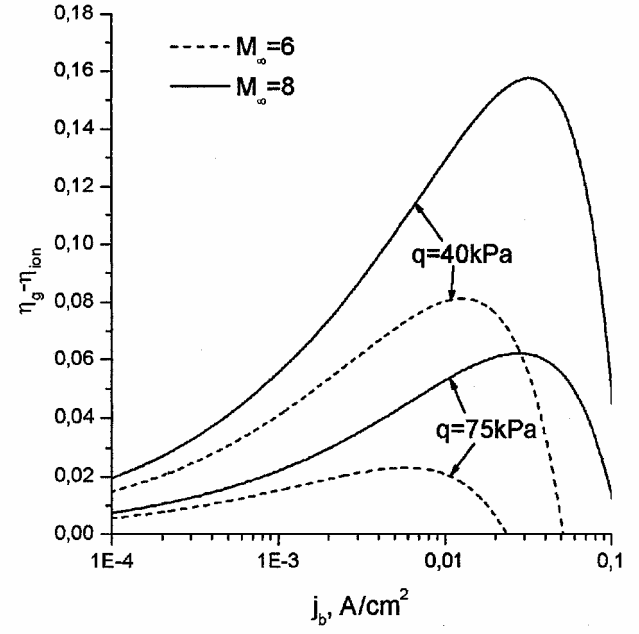

Fig. 13 Relative power excess of MHD generator in MPCE at $M_d = 10$, $\theta_N = 15$ deg, $B = 5$ T, and $k_1 = 0.5$.

inequalities (11). The extent of MHD influence on scramjet performance essentially depends on the parameters of the MHD generator, ionizer, and inlet.

Some results of calculations using dimensional parameters for a scramjet with $\theta_N = 15$ deg, $M_d = 10$, and $F_{\text{th}} = 0.12$ are shown in Figs. 13 and 14. In these calculations we consider the MHD generator with a constant cross-sectional area and e-beam with energy $E_b = 100$ keV as ionizer of flow. Figure 13 shows the dependencies of relative power characteristics of the MHD generator on the current density of e-beam for two values of freestream dynamic pressure q and flight Mach number M_∞. One can see that the power excess $(\eta_g - \eta_{\text{ion}})$ is a nonmonotone function of e-beam current density. At small values of j_b, increasing the current density causes the excess power to be increased too. It is evident that this is because the flow conductivity increases while increasing the current density. At large values of j_b, increasing the current density causes the excess power to decrease. This effect is a consequence of increasing the relative power spent on flow ionization (η_{ion} value). Both increasing the flight Mach number and decreasing the freestream dynamic pressure causes the excess power to increase. Figure 14 shows dependencies of relative specific impulse of the MPCE and relative excess power on j_b for various values of MHD generator length L. These dependencies are similar to ones from the Fig. 13. Increasing the MHD generator length causes the maximum value both for specific impulse and excess power to increase.

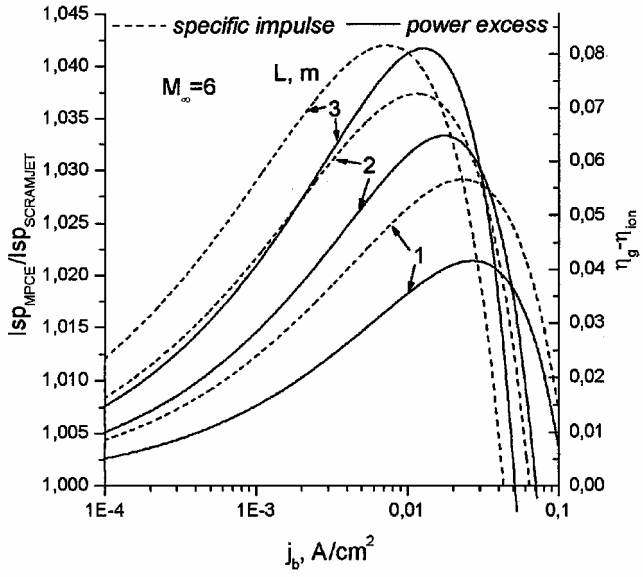

Fig. 14 Relative specific impulse of MPCE and power excess of MHD generator at $M_d = 10$, $\theta_N = 15$ deg, B=5 T, $k_1 = 0.5$, $k_3 = 1.2$, and $q = 40$ kPa.

MHD-Controlled Inlet: Two-Dimensional Analysis

The investigation of an MHD-controlled inlet is carried out in a two-dimensional Euler approach. Stationary flow is considered, such that

$$\frac{\partial \rho v_x}{\partial x} + \frac{\partial \rho v_y}{\partial y} = 0, \qquad \frac{\partial \left(\rho v_x^2 + p\right)}{\partial x} + \frac{\partial \rho v_x v_y}{\partial y} = f_x$$

$$\frac{\partial \left(\rho v_y^2 + p\right)}{\partial y} + \frac{\partial \rho v_x v_y}{\partial x} = f_y$$

$$\frac{\partial (e + p) v_x}{\partial x} + \frac{\partial (e + p) v_y}{\partial y} = q_g + q_r \qquad (12)$$

where $e = \rho[c_v T + (v_x^2 + v_y^2)/2]$ and $p = R\rho T$.

It is assumed that the magnetic induction vector is located in a plane of figure $\boldsymbol{B} = \{B_x, B_y, 0\}$. The density of an induced current $\boldsymbol{j}$ is connected to a magnetic induction vector $\boldsymbol{B}$ and electrical field $\boldsymbol{E}$ by the generalized Ohm's law: $\boldsymbol{j} = \sigma(\boldsymbol{E} + \boldsymbol{v} \times \boldsymbol{B})$. Expressions for the right-hand sides of Eqs. (12) have the following view: $\boldsymbol{f} = \{f_x, f_y, 0\}, \boldsymbol{f} = \boldsymbol{j} \times \boldsymbol{B}$, $q_g = \boldsymbol{j} \cdot \boldsymbol{E}$. The quantity q_r included in the right-hand sides of Eqs. (12) arises from the energy input to a flow as a result of a recombination of charged particles.

We consider the ideally sectioned Faraday MHD generator for which current density has only a z component $[\boldsymbol{j} = (0, 0, j_z)]$. In this case the MHD interaction is defined by the equations $f_x = -j_z B_y$; $f_y = j_z B_x$; $q_g = -j_z k v_\infty B$, where $B = \sqrt{(B_x^2 + B_y^2)}$, and the load factor is determined by the ratio $k = -E_z / v_\infty B$. The MHD generator is characterized by a negative value of q_g; thus, f_x is negative too. One can see that the direction of the y component for the Lorentz force depends on the ratio B_x/B_y. If $B_x/B_y < 0$, then $f_y < 0$, and if $B_x/B_y > 0$, then $f_y > 0$. Thus by changing the direction of the magnetic field, one can change the direction of the

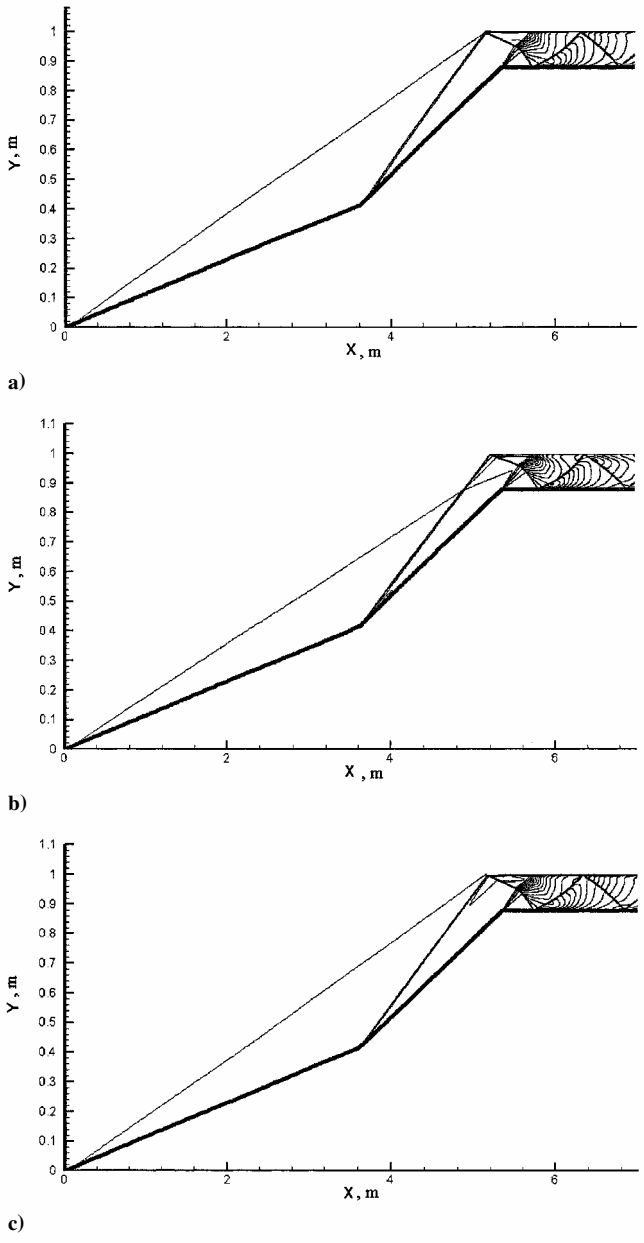

Fig. 15 Density contours in MHD-controlled inlet: a) $M_\infty = M_d = 10$, $B = 0$; b) $M_\infty = 12$, $B = 0$; and c) $M_\infty = 12$, $B = 5.3$ T, $B_x/B_y = 0$.

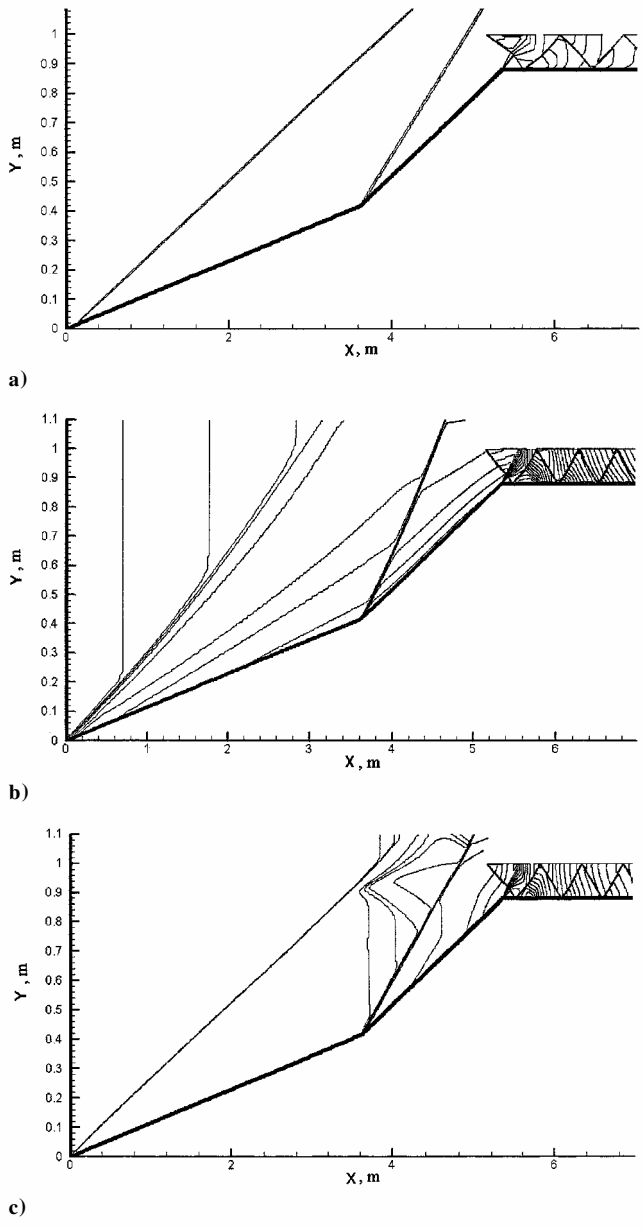

Fig. 16 Density contours in MHD-controlled inlet: a) $M_\infty = 6$, $B = 0$; b) $M_\infty = 6$, $B = 3$ T, $B_x/B_y = 0$, $q_{ion} = 10^{-2}$ W/cm^3, $x_i = 0$, $\Delta x = 5$; and c) $M_\infty = 6$, $B = 3$ T, $B_x/B_y = -1$, $q_{ion} = 1$ W/cm^3, $x_i = 3.5$, $\Delta x = 1$.

Lorentz force. So the MHD interaction in the MHD-controlled inlet will result in flow deceleration ($f_x < 0$) and also in additional compression or depression of the flow caused by the direction of the y component of the Lorentz force.

We consider an inlet with $M_d = 10$ and $\theta_N = 15$ deg, which is shown in Fig. 4. Figure 15a shows density contours in the inlet without MHD interaction at the designed conditions. In this case oblique shocks are concentrated on the cowl lip. Figure 15b shows density contours in the inlet at off-design conditions without MHD interaction, $M_\infty = 12$. In this case points of shocks intersection are not in the cowl lip. Figure 15c shows density contours at $M_\infty = 12$ with MHD interaction, $B = 5.3$ T. One can see that flowfield at off-design conditions with MHD interaction is quite similar to flowfield at design conditions. The same results were obtained in Refs. 7 and 12.

Figure 16 demonstrates the possibility of using an external MHD generator to control the flowfield in an inlet in a situation when the flight Mach number is less than the design Mach number. In this situation the MHD interaction allows one to increase the air mass-flow rate. We consider flight Mach number $M_\infty = 6$, which is noticeably less than the design Mach number. Figure 16a shows density contours in an inlet without MHD control. Figures 16b

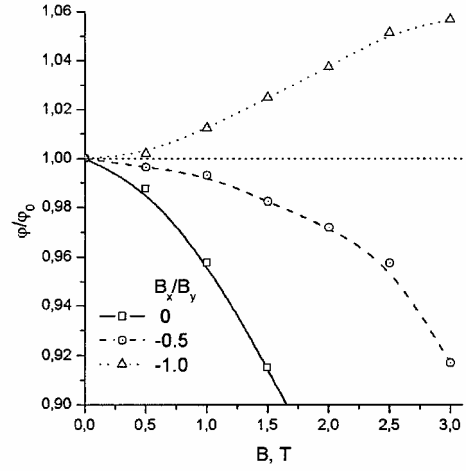

Fig. 17 Relative mass-flow rate at $M_\infty = 6$, $q_i = 10^{-2}$ W/cm^3, $x_i = 0$, and $\Delta x = 5$.

Fig. 18 Relative mass-flow rate at $M_\infty = 6$, $B = 3$ T, and $B_x/B_y = -1$.

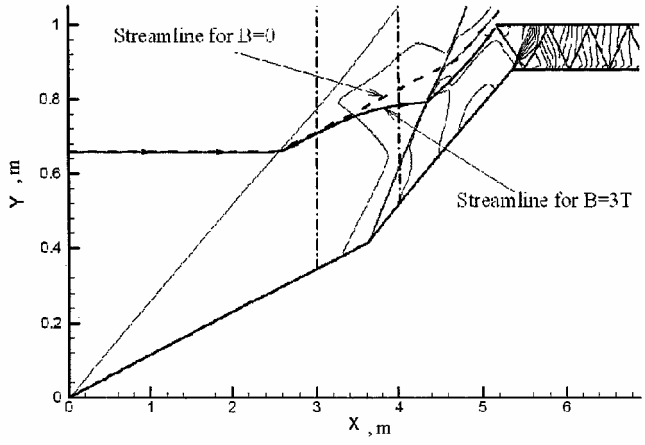

Fig. 19 Density contours in MHD-controlled inlet at $M_\infty = 6$, $B = 3$ T, $B_x/B_y = -1$, $q_{\text{ion}} = 1$ W/cm^3, $x_i = 3$, and $\Delta x = 1$.

and 16c show density contours in an inlet with MHD control. Ionization regions in these cases are infinite bands that are enclosed in the $x_i < x < x_i + \Delta x$ region. Figure 16b demonstrates a flowfield in a MHD-controlled inlet in the case when magnetic induction has only the y component and the ionization region is a broadband. For Fig. 16c the x and y components of the magnetic field are equal, and the ionization region is a narrowband. Figure 17 shows dependencies of the relative value of mass-flow rate upon magnetic induction for various configuration of the magnetic field. Figure 18 shows dependencies of the relative value of the air mass-flow rate on power density put into ionization for various locations of the ionized region. One can see that the configuration and value of magnetic field, location of ionized region, and power density put into ionization noticeably influence the air mass-flow rate. We can conclude that, when the flight Mach number is less than the design Mach number, the effect of MHD interaction depends on many parameters. We can obtain both an increase and a decrease of the air mass-flow rate while increasing the MHD interaction.

Figure 19 illustrates the principle of operation of MHD control, which leads to increasing the air capture in the MHD-controlled inlet. The region of MHD interaction ($3 < x < 4$) is enclosed by dash–dot lines. The streamline for $B = 3$ T, shown in Fig. 19, limits flow region, which is captured in the inlet. In the considered configuration the Lorentz force having the y component, which is directed to the body, distorts the streamline and presses it to the body. It is this effect that increases the air capture and the flow compression. One can see that in the absence of a magnetic field this streamline (dashed line) is not captured in the inlet.

Conclusions

The results obtained show that the MHD generator with nonequilibrium conductivity sustained by an e-beam ionizer allows us to produce electric power at conditions typical for scramjet upstream the combustion chamber. So the MHD generator can be used in a scramjet both for scramjet control and for power producing. The MHD control by internal flow in a scramjet allows one to increase the specific impulse of the scramjet. MHD control by external flow allows one to modify the flowfield in the inlet of the scramjet at off-design conditions. By using the MHD influence on flow, one can control the oblique shock position and air capture in the inlet. In the proper choice of parameters of MHD systems and the ionizer, the MHD control in a scramjet inlet allows us essentially to improve scramjet performance.

Acknowledgment

This work was supported by the European Office of Aerospace Research and Development, ISTC Grant 2088p.

References

[1]Kuranov, A. L., Korabelnicov, A. V., Kuchinskiy, V. V., and Sheikin, E. G., Fundamental Techniques of the 'AJAX' Concept. Modern State of Research," AIAA Paper 2001-1915, April 2001.

[2]Brichkin, D. I., Kuranov, A. L., and Sheikin, E. G., "MHD-Technology for Scramjet Control," AIAA Paper 98-1642, April 1998.

[3]Brichkin, D. I., Kuranov, A. L., and Sheikin, E. G., "The Potentialities of MHD Control for Improving Scramjet Performance," AIAA Paper 99-4969, Nov. 1999.

[4]Kuranov, A. L., Kuchinskiy, V. V., and Sheikin, E. G., "Scramjet with MHD Control Under 'AJAX' Concept. Requirements for MHD Systems," AIAA Paper 2001-2881, June 2001.

[5]Macheret, S. O., Shneider, M. N., and Miles, R. B., "Potential Performance of Supersonic MHD Power Generators," AIAA Paper 2001-0795, Jan. 2001.

[6]"Averaged Energy Required to Produce an Ion Pair," International Commission on Radiation Units and Measurements, Rept. 31, Bethesda, MD, Oct. 1979.

[7]Macheret, S. O., Shneider, M. N., and Miles, R. B., "Energy-Efficient Generation of Nonequilibrium Plasmas and Their Applications to Hypersonic MHD Systems," AIAA Paper 2001-2880, June 2001.

[8]"The Calculation of Electrokinetic Properties of Air and Nitrogen Plasma Excited by e-Beam," Hypersonic System Research Inst., Rept. 87-615/171, St. Petersburg, Russia, Dec. 1995 (in Russian).

[9]Macheret, S. O., Shneider, M. N., and Miles, R. B., "MHD Power Extraction from Cold Hypersonic Air Flow with External Ionizer," AIAA Paper 99-4800, Nov. 1999.

[10]"Stopping Powers for Electrons and Positrons," International Commission on Radiation Units and Measurements, Rept. 37, Bethesda, MD, Oct. 1984.

[11]Brichkin, D. I., Kuranov, A. L., and Sheikin, E. G., "Scramjet with MHD Control Under 'AJAX' Concept. Physical Limitations," AIAA Paper 2001-0381, Jan. 2001.

[12]Golovachev, Y. P., and Suschikh, S. Y., "Weakly Ionized Flows in Supersonic Inlets Subjected to the External Electromagnetic Fields," *Perspectives of MHD and Plasma Technologies in Aerospace Applications*, edited by V. A. Bityurin, Inst. of High Temperatures, Russian Academy of Sciences, Moscow, 1999, p. 105.

I. D. Boyd
Associate Editor